ACS APPLIED MATERIALS & INTERFACES

Forum Article

www.acsami.org

Electrical Potential-Assisted DNA Hybridization. How to Mitigate Electrostatics for Surface DNA Hybridization

Jakub Tymoczko, Wolfgang Schuhmann, and Magdalena Gebala*,†

Analytical Chemistry, Center for Electrochemical Sciences (CES), Ruhr-Universität Bochum, Universitätsstrasse 150, 44780 Bochum, Germany

ABSTRACT: Surface-confined DNA hybridization reactions are sensitive to the number and identity of DNA capture probes and experimental conditions such as the nature and the ionic strength of the electrolyte solution. When the surface probe density is high or the concentration of bulk ions is much lower than the concentration of ions within the DNA layer, hybridization is significantly slowed down or does not proceed at all. However, high-density DNA monolayers are attractive for designing high-sensitivity DNA sensors. Thus, circumventing sluggish DNA hybridization on such interfaces allows a high surface concentration of target DNA and improved signal/noise ratio. We present potential-assisted hybridization as a strategy in which an external voltage is applied to the ssDNA-modified interface during the hybridization process. Results show that a significant enhancement of hybridization can be achieved using this approach.

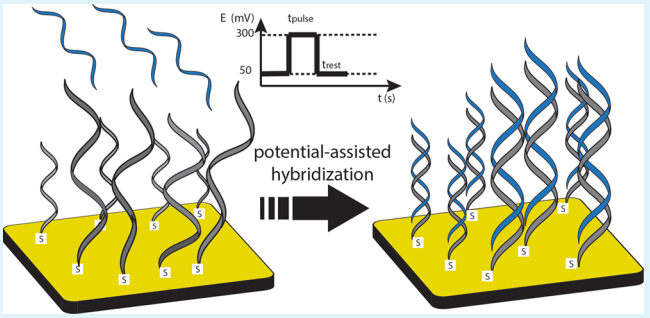

KEYWORDS: *DNA, potential, intercalator, DNA hybridization, hybridization acceleration, self-assembled monolayer*

INTRODUCTION

A DNA sensor consists of a single-stranded (ss)DNA probe grafted at a transducer surface that serves as a recognition element for hybridization of a complementary DNA target strand. This recognition process caused by the formation of Watson−Crick base pairs through multiple hydrogen bonds has then to be converted into a measurable signal. Evidently, the signal transduction process has to be capable of differentiating between single-stranded and double-stranded (ds)-oligonucleotides at the interface. This is commonly achieved by the use of hybridization indicators[1−3] or through changes in the physicochemical properties of the sensing layer induced by the complementary binding event.[4−8] The main challenge, however, is to define the optimum conditions for fast and maximum hybridization efficiency in order to obtain a highly sensitive DNA assay.

The hybridization is affected by surface probe coverage (Γ_{max}) and ion concentration present in the hybridization solution.[9−14] At low Γ_{max}, high hybridization efficiency is reached because electrostatics and the exclusion volume effects are minimized. The surface concentration of the formed dsDNA (Γ_p) is limited by the surface-tethered DNA capture probe density that is far below 1×10^{12} molecules/cm^2. The small amount of dsDNA after hybridization may lead to a poor signal-to-noise ratio and hence an insufficient detection limit. A possible way to improve the signal-to-noise ratio is either by using signal amplification strategies or it can be achieved by increasing the surface-bound capture DNA probe density. However, as the DNA density at the interface increases intermolecular interactions between the DNA strands within the monolayer become stronger and the complexity of this situation is even further increased upon insertion of additional DNA chains while the hybridization process proceeds.[13,14] Thus, hybridization kinetics slows down and the hybridization efficiency decreases because of enhanced electrostatic interactions and steric crowding. At high-density DNA interfaces, a negative electric field is built-up that repels target DNA molecules approaching from solution. Thus, mitigating this electric field may significantly improve hybridization kinetics and as a consequence lead finally to a higher surface concentration of dsDNA and a higher detection signal. One possible approach that has recently received considerable interest is to circumvent the slowdown of hybridization at high-density DNA monolayers by applying an external voltage while hybridization proceeds.[14−20]

In this work, we investigate potential-assisted hybridization by applying a constant potential or sequences of potential pulses. Hybridization at high probe DNA density is characterized by a 2 orders of magnitude higher dissociation constant (k_{off}) and a 1 order of magnitude lower association constant (k_{on}) as compared with interfaces with low probe DNA density. Applying the external potential enhances k_{on} but does not have any effect on k_{off}. These results imply that dsDNA in a dense monolayer is less stable as compared to hybridization at low probe DNA density monolayers. However,

Special Issue: Materials for Theranostics

Received: May 6, 2014
Accepted: July 29, 2014
Published: August 7, 2014

   dx.doi.org/10.1021/am5027902 | *ACS Appl. Mater. Interfaces* 2014, 6, 21851−21858

Scheme 1. (A) Schematic Representation of the Sequential Build-up of the DNA-Modified Recognition Interface Including Its Characterization and Hybridization with the Complementary Ferrocene-Tagged Target DNA; (B) Schematic Representation of the Potential Pulses over Time Used for Potential-Assisted DNA Hybridization

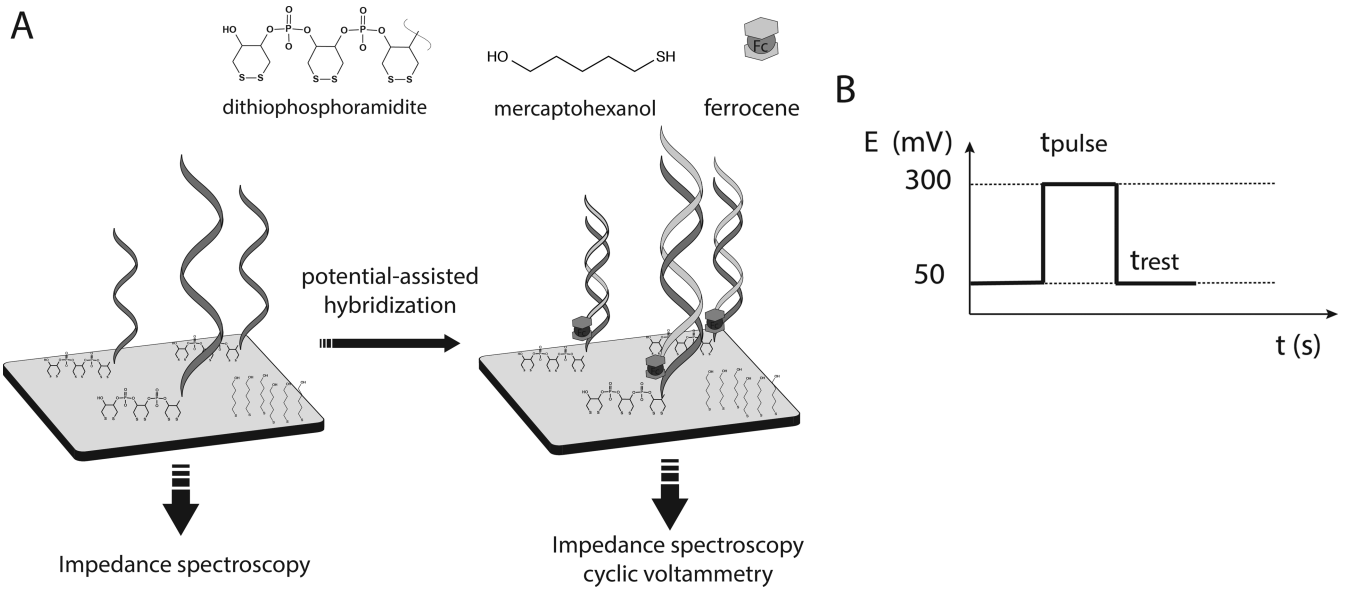

high dsDNA surface coverage can be achieved using potential-assisted hybridization preferentially by applying optimized potential pulse sequences ensuring a proper orientation of DNA molecules at the electrified interface.

2. EXPERIMENTAL SECTION

2.1. Materials and Reagents. DNA oligonucleotides were purchased from FRIZ Biochem (Neuried, Germany). DNA capture probe (20-mer): 3′−OH-(dithiophosphoramidite)$_3$-hexaethylenglycol-$(CH_2)_3$−TCC ACT GAC ACA ATA GGC GT 5′; complementary DNA target: 3′ ACG CCT ATT GTG TCA GTG GA-(F_C) 5′. Ethanol was from Merck (Darmstadt, Germany), KH_2PO_4 from VWR international (Darmstadt, Germany), K_2HPO_4 from Fischer Chemical (Schwerte, Germany), H_2SO_4 from J.T. Baker (Deventer, The Netherlands), 6-mercaptohexan-1-ol (MCH) from Fluka Chemie (Buchs, Switzerland), KF·2H_2O from Sigma-Aldrich Chemie (Steinheim, Germany). All reagents were of analytical grade and used as received.

2.2. Preparation of Electrodes and DNA Immobilization. Polycrystalline gold electrodes (2 mm diameter, CH Instruments, Austin, USA) were polished with wet alumina slurries with particles sizes of 0.3 and 0.05 μm (Leco, St. Joseph, USA) on polishing cloths (Heraeus, Wehrheim, Germany). Afterward, the electrodes were rinsed with water and electrochemically characterized by means of cyclic voltammetry (CV) in 0.5 M H_2SO_4 in a potential range from 0 V to +1.2 V vs Ag/AgCl (3 M KCl) at a scan rate of 100 mV s^{-1} until a stable voltammogram was obtained. The roughness factor of the electrodes was determined as the ratio of the real area A_{real} to the geometric area $A_{geometric}$ of an electrode, where A_{real} is the microscopic surface area obtained by estimation of the charge transferred during reduction of gold oxide and dividing it by 482 μC/cm^2. The roughness factors were typically in the range of 1.23−1.28.

After electrochemical cleaning, the electrodes were characterized by electrochemical impedance spectroscopy (EIS) and subsequently used to tether DNA capture probes. Immobilization of DNA was carried out initially for 2 h in 1 mM phosphate buffer solution containing 600 mM K_2SO_4, pH 7.0, at a temperature of 36 °C controlled by a heating thermomixer (HTC BioTech, Ditabis, Germany). Subsequently, the electrodes were thoroughly rinsed with phosphate buffer to remove any excess of reagents or any loosely bound DNA strands, characterized by EIS and afterward dipped again into the immobilization solution for another 1 h. In this way, stable and reproducible DNA monolayers were obtained. To complete the preparation, the ssDNA-modified electrodes were immersed into a buffered solution containing 10 mM mercaptohexan-1-ol (MCH) and this leads to formation of binary monolayers of the DNA capture probe and MCH.

2.3. Complementary DNA Hybridization. The potential assisted DNA hybridization process was carried out in 1 mM phosphate buffer, pH 7.2, containing either 20 mM or 450 mM K_2SO_4, respectively. The concentration of DNA target molecules was kept at 1 μM and the volume of the hybridization solution was 1 mL. Hybridization was carried out by applying either a constant potential of +300 mV vs Ag/AgCl (3 M KCl) or a pulsed variation of two potentials (+300 mV and +50 mV). When the potential pulses were used, the impact of the duration of these pulses was studied as well.

Complementary DNA molecules used in these studies were tagged at the 5′ end with a redox marker, ferrocene ($Fc^{0/+}$). Upon hybridization the DNA-bound ferrocene moieties were located at the bottom of the mixed DNA/MCH monolayer. Tagging DNA with the redox probe allowed determination of the DNA surface concentration (Γ_p) after hybridization. To do so, the charge (Q) transferred during the oxidation or the reduction of ferrocene moieties was evaluated. The relation between the recorded charge and the surface concentration was expressed by $\Gamma = Q/nFA_{real}$ (n = number of electrons; F = Faraday constant; A_{real} = microscopic surface area of the bare gold electrode). Because there was one ferrocene moiety per dsDNA, the estimated surface concentration of the redox probes was equal to the surface concentration of the dsDNA (Γ_p). To record the transferred charge for the $Fc^{0/+}$ redox process, cyclic voltammograms in the potential range of −50 mV to 500 mV vs Ag/AgCl (3 M KCl) were performed at a scan rate of 10 V s^{-1} in phosphate buffer (1 mM KH_2PO_4 /K_2HPO_4; pH 7.0) containing 500 mM KF. The choice of KF as supporting electrolyte was suggested by the fact that F^- ions exhibit low affinity toward gold surfaces thus allowing a rigorous electrochemical characterization of the redox probe surface coverage.[21]

2.4. Electrochemical Impedance Spectroscopy. Electrochemical impedance measurements were performed at the equilibrium potential of the redox couple $K_3[Fe(CN)_6]/K_4[Fe(CN)_6]$ (+250 mV vs Ag/AgCl/3 M KCl), at equimolar concentration of 5 mM each, prepared in 10 mM phosphate buffer, pH 7.2, containing 20 mM K_2SO_4. A standard three-electrode configuration was used, that consisted of a Ag/AgCl (3 M KCl) reference electrode, a platinum wire auxiliary electrode and a bare or modified Au working electrode.

dx.doi.org/10.1021/am5027902 | ACS Appl. Mater. Interfaces 2014, 6, 21851−21858

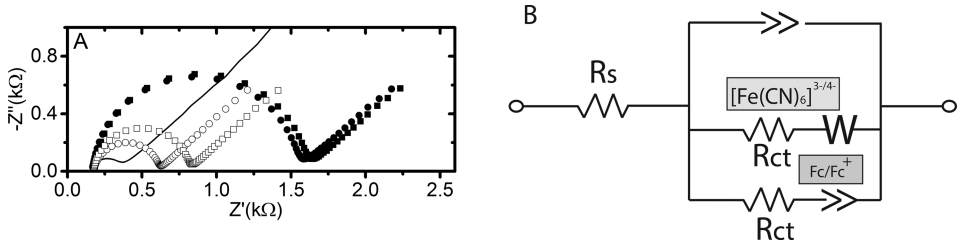

Figure 1. (A) Impedance spectra (Nyquist plots) for the ssDNA/MCH-modified gold electrode (closed symbols). Upon potential-assisted hybridization at a constant potential of +300 mV for 35 min using the Fc-tagged target-DNA molecules, the corresponding EIS with open squares (□) at low ionic strength and open circles (○) at high ionic strength are obtained. The solid line shows EIS of an unmodified gold electrode. (EIS recorded in 5 mM $[Fe(CN)_6]^{3-/4-}$ buffered solution at a DC potential of 250 mV vs Ag/AgCl (3 M KCl); applied AC perturbation: 5 mV_{pp}. Frequency range from 30 kHz to 0.1 Hz). (B): Equivalent circuit representing the interface after DNA hybridization.

Measurements were carried out at a constant DC potential (+250 mV vs Ag/AgCl) which was superimposed by an AC perturbation with an amplitude of 5 mV_{pp}. The AC modulation frequency was swept down from 30 kHz to 0.1 Hz with 10 measuring points per decade in logarithmic distribution. Electrochemical impedance spectra (EIS) were recorded using a μAutolab III potentiostat equipped with a frequency response analyzer (FRA) (Metrohm-Autolab, Utrecht, The Netherlands). Data evaluation was performed using OriginPro8G (OriginLab, Northampton, USA).

3. RESULTS

Scheme 1 presents the overall strategy how to prepare a reproducible DNA recognition interface and to carry out and study the proposed potential-assisted hybridization strategy. The DNA capture probes were modified at their 3′ end with three dithiophosphoramidite units which ensured a highly stable linkage of the DNA to the surface of the gold electrode through the formation of 6 gold−sulfur bonds per DNA molecule. Upon subsequent modification with mercaptohexanol (MCH) the tethered ssDNA molecules formed a highly reproducible recognition interface. As suggested from the EIS characterization, the DNA/MCH-modified gold electrodes had a similar amount of tethered molecules represented by a narrow distribution of less than 3% of the measured capacitance as well as charge-transfer resistances (R_{ct}). The same surface coverage is an indispensable prerequisite to investigate the impact of the potential-assisted hybridization. The influence of the applied potential has been studied either by applying a constant potential of +300 mV or a repetitive sequence of two potentials pulses of +300 mV and +50 mV. The potential of +300 mV is called the active pulse potential (E_p), whereas the potential of +50 mV is called the resting potential (E_r). The duration for applying these potentials was varied as well, either by keeping the duration of the active pulse potential constant (1 s) and shortening the time of the resting potential from 30 to 1 s or by shortening both to 0.1 s. Potential-assisted hybridization was compared to hybridization carried out in a solution without applying any potential. The overall time for all hybridization procedures was kept constant (35 min).

As a matter of fact, the active pulse potential should be substantially higher than the potential of zero charge (PZC) of the modified electrode surface in order to ensure an excess of positive charges at the electrified interface. The PZC is considered to be ∼100 mV (vs Ag/AgCl).[22] At the same time, the active pulse potential has to be kept below the onset potential of the gold−sulfur bond oxidation.

The 5′ end of the target DNA was modified with the ferrocene redox marker and this allowed for monitoring the hybridization efficiency by intermittently recorded fast scan cyclic voltammetry FSCVs and/or EIS. Upon hybridization the ferrocene moieties were introduced into the dsDNA monolayer and placed in close proximity to the electrode surface (see Scheme 1). The electron-transfer rate of the redox couple was negligibly affected by molecular motions of the dsDNA like rotational dynamics[23] or elastic bending of dsDNA.[24] Hence, this configuration ensured a reproducible determination of the surface coverage with dsDNA.[21,25]

3.1. Potential-Assisted Hybridization at a Constant Potential. *3.1.1. Surface Characterization by Means of Electrochemical Impedance Spectroscopy.* At first, potential-assisted hybridization was carried out at a constant potential of +300 mV vs Ag/AgCl (3 M KCl). When a potential substantially higher than the PZC is applied to the interface a positive electric field arises in front of the electrode. The negatively charged DNA target strands which are in close proximity to the electrified interface feel electrophoretic forces toward the interface which may affect hybridization. The strength of this interaction depends supposedly on the ionic conditions, i.e., the concentration of the supporting electrolyte and the applied potential. To evaluate the impact of the concentration of the background electrolyte, we performed potential-assisted hybridization experiments at low (10 mM K_2SO_4) and high (450 mM K_2SO_4) ionic strength conditions. Because the progress of the hybridization process was monitored intermittently at predefined time intervals, information about kinetics and thermodynamics could be obtained.

Properties of the ssDNA/MCH-modified gold electrode surface have to be known prior to potential-assisted hybridization. EIS in the presence of a free-diffusing and charged redox couple allows evaluating how the redox process of e.g. the negatively charged $[Fe(CN)_6]^{3-/4-}$ is modulated upon altering the properties of the electrified interface by immobilized DNA molecules. Figure 1 represents EIS of the initial status of the interface, the bare gold electrode (solid line) and the ssDNA/MCH monolayer modified electrode (closed symbols), as well as the interface after hybridization under formation of a dsDNA/MCH modified surface (open symbols). The significant increase in the charge-transfer resistance from the bare to the ssDNA/MCH modified surface is in accordance with a decrease in the electron-transfer rate of the redox reaction of $[Fe(CN)_6]^{3-/4-}$.

Independently prepared electrodes showed very small differences of less than 3% in the R_{ct} values indicating high reproducibility of the ssDNA/MCH monolayer formation. Upon potential-assisted hybridization for 35 min at a constant applied potential of +300 mV using the Fc-tagged target DNA strands, a substantial decrease of R_{ct} was observed in both cases,

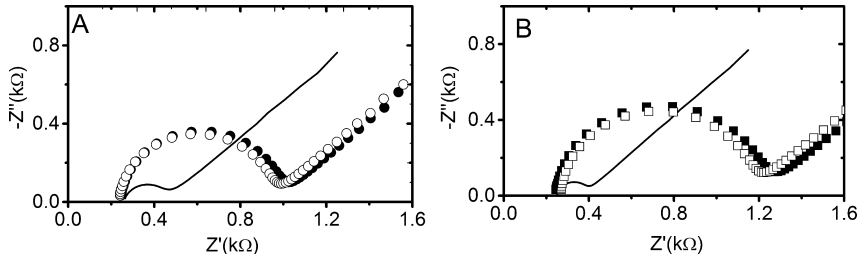

Figure 2. Impedance spectra (Nyquist plots) for an unmodified gold electrode (solid line), MCH modified electrode (●) and ssDNA/MCH modified electrode (■). (A) Potential-assisted hybridization carried out at the MCH-modified interface without any DNA capture probes at a constant potential of +300 mV for 35 min (○). (B) Potential-assisted hybridization carried out at the ssDNA/MCH-modified interface at a constant applied potential of −300 mV for 35 min (□). (EIS recorded in 5 mM $[Fe(CN)_6]^{3-/4-}$ buffered solution at a DC potential of 250 mV vs Ag/AgCl (3 M KCl); applied AC perturbation: 5 mV_{pp}. Frequency range from 30 kHz to 0.1 Hz).

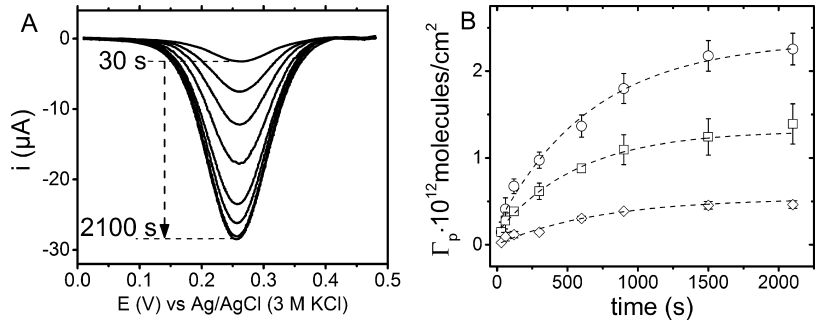

Figure 3. Characterization of the dsDNA/MCH monolayer during potential-assisted hybridization. (A) Series of FSCV of Fc-tagged dsDNA reduction representing the kinetics of the hybridization process. (B) Hybridization kinetics for hybridization at open-circuit potential (◊), the potential-assisted hybridization at low ionic strength (constant potential of +300 mV; 1 mM phosphate buffer with 10 mM K_2SO_4, pH 7.4; □), and high ionic strength (constant potential of +300 mV; 1 mM phosphate buffer with 450 mM K_2SO_4, pH 7.4;○). All data were fitted to the first-order Langmuir isotherm function (dashed line).

when hybridization was carried out at low and high ionic strength conditions. However, if the potential-assisted hybridization was carried out at the low ionic strength (1 mM phosphate butter containing 10 mM K_2SO_4, pH 7.4; □) the R_{ct} was higher as compared to hybridization at the higher salt concentration (1 mM phosphate butter containing 450 mM K_2SO_4, pH 7.4; ○). At longer hybridization times, no further changes in the corresponding EIS could be observed (data not shown).

An unconventional way of acquiring EIS characterization of DNA modified interfaces was performed, since two redox mediators were simultaneously present during measurements. Usually, the faradaic impedance is recorded for an equimolar mixture of $[Fe(CN_6)_3]^{3-/4-}$. Here, in addition to the $[Fe(CN_6)_3]^{3-/4-}$ couple, ferrocene moieties ($Fc^{0/+}$) were present at the interface. The redox reactions of the diffusive $[Fe(CN_6)_3]^{3-/4-}$ couple and the surface confined $Fc^{0/+}$ were considered as parallel processes. Due to the very close formal potentials of the $[Fe(CN_6)_3]^{3-/4-}$ couple (250 mV) and the $Fc^{0/+}$ couple (280 mV) both redox reactions were indistinguishable during EIS measurements. In this way, additional redox reactions occurred at the interface as compared to EIS measurement with only one redox couple, which was considered to be the main reason for the substantially decreased overall R_{ct} after potential-assisted hybridization. The Randle's equivalent circuit was hence modified to represent two parallel pathways as shown in Figure 1B. However, because EIS was intended only to acquire a qualitative description of the interface and to evaluate the reproducibility of the sequential built-up of the interface, the exact electron-transfer mechanism was not further investigated.

Figure 2 shows Nyquist plots of control EIS experiments. The first control experiment (Figure 2A) interrogated the nonspecific adsorption of target molecules when a positive electric field was built up at the electrode. For this, an electrode surface only modified with a MCH (●) monolayer was subjected to the potential-assisted hybridization with the Fc-tagged target DNA strands at a constant potential of +300 mV. As expected, due to the absence of the capture probe no Fc-tagged dsDNA (○) was accumulated at the interface leading to an unchanged R_{ct} value.

The second control experiment evaluated the influence of an applied potential that is below the PZC. In this case, an electrode modified with the ssDNA/MCH monolayer (■) was exposed to the Fc-tagged target DNA strand while applying a constant potential of −300 mV (Figure 2B). Again no Fc-tagged dsDNA (□) was accumulated at the interface leading to an unchanged R_{ct} value suggesting unfavorable conditions for a productive hybridization. The presence of the ssDNA capture strands was clearly visible in the higher R_{ct} of the ssDNA/MCH modified surface in Figure 2B (■) as compared with the only MCH-modified surface in Figure 2A (●).

3.1.2. Surface Characterization: Cyclic Voltammetry of Fc-Tagged dsDNA Monolayers. Fast-scan cyclic voltammetry (FSCV) was carried out in 1 mM phosphate buffer containing 500 mM KF in a potential range in which the monolayers are stable (−50 to +550 mV vs Ag/AgCl/3 M KCl). The FSCV data were acquired as a triple scan at a given scan rate to obtain reliable data of the equilibrated system. The charge extracted from the integration of the faradaic currents remained stable independent of the direction and the speed of the potential scans which confirmed the stability of monolayers. Figure 3A

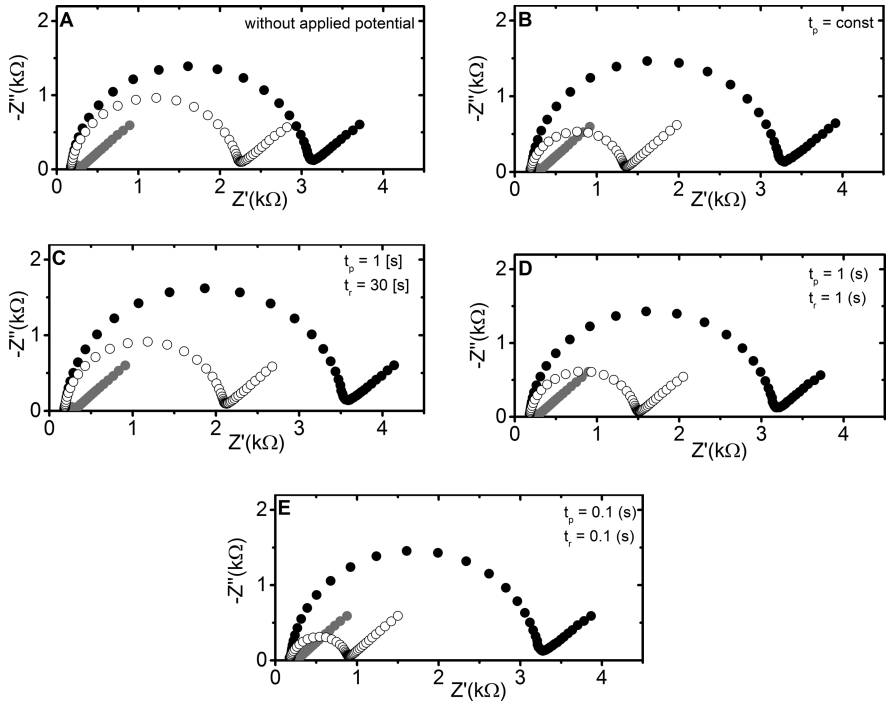

Figure 4. Nyquist plots of ssDNA/MCH-modified Au before (•) and after 35 min hybridization with the Fc-tagged target DNA (1 μM) using different potential-pulse sequences for potential-assisted hybridization (○). The gray dots are representing the bare Au electrodes. Hybridization was carried out in 1 mM phosphate buffer containing 450 mM K_2SO_4, pH 7.4. A) without applying an external potential. B) applying a constant external potential of +300 mV. C - E) applying potential pulse sequences of various durations of t_p and t_r as indicated in the figures. (EIS recorded in buffered solution of 5 mM $[Fe(CN)_6]^{3-/4-}$ at a DC potential of 250 mV vs Ag/AgCl (3 M KCl); applied AC perturbation: 5 mV_{pp}. Frequency range from 30 kHz to 0.1 Hz).

presents the reduction current of Fc^+ after background current subtraction recorded at the specified time after starting potential-assisted hybridization.

Evidently, the charge continuously increased during the course of potential-assisted hybridization. It indicates the formation of Fc-tagged dsDNA at the biorecognition interface. The current stabilized after about 35 min that suggested that no further hybridization took place after this time. By integrating the reduction currents and taking into account the scan rate at which the voltammograms were recorded, the charge transferred during the reduction of Fc^+ could be determined as a basis for deriving the target DNA surface coverage (Γ_p). The increasing surface coverage Γ_p plotted as a function of time provided clear differences in dependence from the hybridization conditions. The standard hybridization technique when the ssDNA/MCH-modified surface was immersed in a buffered solution containing 1 μM of the Fc-tagged target DNA without applying any external potential reached a surface coverage Γ_p of $4.7 \pm 0.67 \times 10^{11}$ molecules/cm^2. Because all ssDNA/MCH-modified electrodes exhibited a similar coverage with DNA capture probes as indicated by EIS, one could conclude that immersion of the electrode into the target DNA strand containing solution yielded only 21% of the total hybridization efficiency as compared to potential-assisted hybridization. When hybridization was carried out by generating the electric field through a constant potential of +300 mV, the number of surface-bound dsDNA was substantially increased. However, there was a clear difference if the potential-assisted hybridization was carried out at the high or the low ionic strength. At low ionic strength (1 mM phosphate buffer containing 10 mM K_2SO_4), a surface coverage Γ_p of 1.4 ± 10^{12} molecules/cm^2 was obtained, whereas at the high ionic strength (1 mM phosphate buffer containing 450 mM K_2SO_4), the surface coverage was 2.3 ± 10^{12} molecules/cm^2.

3.2. Potential-Assisted Hybridization by Modulation of the Electric Field through Potential Pulses. From the results obtained at a constant applied potential higher than PZC, it became clear that potential-assisted hybridization improves hybridization efficiency as well as hybridization kinetics. In the following, we want to develop insight into how the duration of the applied potential affects hybridization. For this, we carried out potential-assisted hybridization experiments while modulating the electric field at the interface by means of sequences of potential pulses. The potential pulses were defined by the active pulse potential (E_p = +300 mV) applied for the active pulse time t_p and the resting potential (E_r = +50 mV) applied for the resting time t_r. We evaluated the following potential-pulse profiles: (a) t_p = 1 s and t_r = 30 s or 1 s, respectively; (b) t_p and t_r = 0.1 s.

Figure 4 shows electrochemical impedance spectra of the modified surfaces obtained after potential-assisted hybridization applying the mentioned potential-pulse profiles during hybridization for 35 min. Again, as can be derived from the R_{ct} values of the ssDNA/MCH-modified surfaces, all electrodes exhibited a similar capture DNA probe surface coverage. As expected, the application of the different potential profiles affects substantially hybridization efficiency and evidently the relative duration t_p and t_r of the applied potentials E_p and E_r are important. As can be derived qualitatively from the impedance measurements (Figure 4) the hybridization efficiency was not substantially improved when the resting potential was considerable longer than the active pulse potential (Figure 4C) as compared with the standard hybridization conditions without applying a potential (Figure 4A). When t_r or both, t_p and t_r were

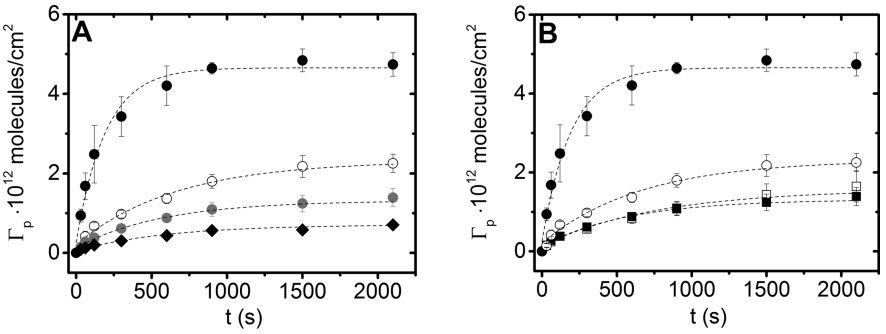

Figure 5. Hybridization kinetics. (A) Potential-assisted hybridization at high ionic strength (1 mM phosphate buffer containing 450 mM K_2SO_4) at a constant potential of +300 mV (○) and potential pulse sequences with the amplitude of 250 mV and various durations of the active potential (t_a) and resting potential (t_r): (●) t_a = 0.1 s and t_r = 0.1 s, (gray solid circle) t_a = 1 s and t_r = 1, (♦) t_a = 1 s and t_r = 30 s. B) Potential-assisted hybridization at high ionic strength (○) and low ionic strength (□; 1 mM phosphate buffer containing 10 mM K_2SO_4) at a constant potential of +300 mV. Potential pulse sequences with the amplitude of 250 mV and t_a = 0.1 s and t_r = 0.1 s at high ionic strength (●) and low ionic strength (■). All data were fitted to the first-order Langmuir isotherm function (dashed line).

decreased the hybridization efficiency increased and R_{ct} after hybridization (○) was considerably lower (Figure 4D). Moreover, the electric field generated by potential pulses had a stronger impact on the hybridization efficiency than the constant application of a suitable potential (compare Figure 4C, E).

An alternative way to visualize the obtained data presented in Figure 4 is as hybridization kinetics shown in Figure 5. The surface concentration of the Fc-tagged target DNA (Γ_p) was plotted as a function of hybridization time. The highest coverage of dsDNA molecules was obtained when the applied potential was continuously pulsed between the resting potential of +50 mV and the active pulse potential of +300 mV with equal t_p and t_r at a frequency of 10 Hz. For the hybridization at low ionic strength conditions no improvement in the hybridization rate or efficiency were revealed as compared to hybridization at constant potential (Figure 5B (■) and (□)). These results again suggest a strong impact of the concentration of ions present in the solution and at the interface on the efficiency of DNA hybridization.

4. DISCUSSION

When the hybridization of a target DNA with a complementary surface-confined DNA capture probe is carried out at an excess of the target DNA strands the limiting step is considered to be independent of the diffusional mass transport of the target strands to the surface and the recognition event itself becomes rate limiting. In this case, the hybridization can be treated as a first-order Langmuir isotherm, which can be solved analytically (eq 1)

$$\theta = \frac{KC^T}{1 + KC^T}[1 - e^{-t/\tau}] \quad (1)$$

where θ is the surface coverage defined as the ratio $\theta = \Gamma_p/\Gamma_{max}$. Γ_p is the surface concentration of the target, here the dsDNA, whereas Γ_{max} is the concentration of adsorption sites, representing the initial concentration of immobilized capture DNA probes available for adsorption. K is the equilibrium constant $K = k_{on}/k_{off}$, C^T is the concentration of target DNA in solutions (C^T = 1 μM), and τ is the time constant defined as (eq 2)

$$\tau = \frac{1}{k_{on}C^T + k_{off}} \quad (2)$$

DNA hybridization at low density monolayers, i.e., $\Gamma_{max} \leq 1 \times 10^{12}$ molecules/cm^2 is characterized by 100% efficiency with rate constants $k_{on,dilute} \approx 1 \times 10^4$ M^{-1} s^{-1} and $k_{off,dilute} \approx 1 \times 10^{-5}$ s^{-1}.[14] However, increasing the concentration of the adsorption sites (Γ_{max}) considerably slows down hybridization kinetics. At intermediate concentrations $\Gamma_{max} \approx 1 \times 10^{13}$ molecules/cm^2 the hybridization efficiency drops down to a level of about 40% or less depending on ionic strength conditions.[13] According to Levicky's terminology this intermediate concentration is called suppressed hybridization regime (SH) while the low concentration is called the pseudo Langmuir regime (PL). No hybridization is observed for monolayers of $\Gamma_{max} \approx 3 \times 10^{13}$ molecules/cm^2 (no hybridization-NH regime). Because in this work the capture DNA probe density is about 5×10^{12} molecules/cm^2, we assume for the following consideration that the SH regime is valid. Low surface densities are not investigated in this work, because it is known that 100% hybridization efficiency is observed in these cases even without potential-assisted hybridization and no enhancement of DNA surface hybridization should be observed for the potential-assisted hybridization.

As a result of increasing Γ_{max}, the electrostatic potential within the DNA monolayer rises significantly, hence slowing down hybridization kinetics. The complexity of this situation further increases as additional DNA chains insert into the monolayer while hybridization proceeds. Concomitantly, the activation energy (ΔG_a) of the DNA hybridization, which is already much higher for dense DNA monolayers as compared to diluted ones, increases even more when DNA duplexes are formed because of electrostatic and steric interactions.

A way to decrease the activation barrier for high density monolayers is to mitigate the electrostatic potential within the layers. However, the electrostatic energy cannot be easily compensated by mobile ions. Melosh et al. proposed a model according to which high density monolayers (SH and NH regime) lack of mobile ions. DNA molecules together with their hydration shells and the surrounding condensed ions occupy a significant volume within these high-density layers thus excluding additional mobile ions.[14] By applying an external potential, one can reduce the electrostatic barrier and increase the hybridization efficiency to the level characteristic for diluted monolayers.[14]

All experiments presented above were fitted to the first-order Langmuir isotherm despite of the comparatively high surface

coverage. The dissociation constants in all cases, with and without applying a potential during hybridization, were the same and about 2 orders of magnitude higher than the dissociation constant of a diluted DNA monolayer ($k_{off,dilute}$). Hence, the formed dsDNA were less stable, seemingly because of the increased electrostatic potential within the layer. At the same time, the association constant for hybridization carried out without applying any external potential was about 1 order of magnitude lower, $k_{on} \approx 1 \times 10^3$ M^{-1} s^{-1} vs $k_{on,dilute} \approx 1 \times 10^4$ M^{-1} s^{-1}. However, when a constant external potential was applied, k_{on} increased to a value of 7.5×10^3 M^{-1} s^{-1}, and for potential-assisted hybridization carried out with t_p and t_r of 0.1 s each, k_{on} is 4×10^4 M^{-1} s^{-1} This increase in k_{on} for potential pulse assisted vs constant potential hybridization suggests that the externally applied potential affects the DNA orientation at the surface. Though the ssDNA surface density is comparatively high and it is expected that the DNA strands are favoring upward orientation[26] some rearrangements may still occur. It is not anticipated that the surface-tethered DNA molecules switch from lying down on the surface to a fully extended conformation while the voltage is pulsed from positive (above PZC) to negative (below or close to PZC),[27] but rather a sort of induced intermolecular interactions occurs leading to a decreasing accessibility of the DNA capture probes for hybridization. These interactions presumable last longer when a constant potential is applied generating a constant electric field. At high ssDNA surface coverage when no external electric field is applied, the DNA chains behave more like fully extended, rigid rods due to strong electrostatic repulsions within the monolayer. In other words, there are two substantially different states in which grafted DNA molecules are electrostatically trapped (no relaxation). On the one side, a negative electric field arising from the high Γ_{max} and the lack of mobile ions leads to upward orientated DNA molecules. On the other side, a positive electric field generated by the applied external voltage results in enhanced intermolecular interactions. Switching between these two scenarios may be the reason for the improved hybridization kinetics. Therefore, potential-pulse assisted hybridization show a much higher Γ_p as compared with the application of the constant potential. However, this is true only when a proper pulse duration is ensured. If the resting potential E_R (here +50 mV) at which the capture probes are electrostatically trapped in upward configuration thus improving their accessibility to the target DNA molecules lasts longer than the potential mitigating the electrostatic barrier of hybridization, hybridization kinetics are slow and similar to standard hybridization without any applied potential. When t_r is shortened to 1 s becoming the same as t_p, hybridization improved but did not become better than hybridization at the constant potential. Only when both t_p and t_r are set to 0.1 s a significant improvement in the hybridization efficiency was observed. Rant and co-workers showed that the transition of surface-tethered ssDNA in a diluted monolayer from the lying down on the surface to the upward orientation takes about 250 μs.[28] This DNA motion is correlated to the double-layer formation that is a function of solution properties (ion concentration) and the size of the electrode. Because we have used substantially higher ssDNA probe concentration we anticipate much longer transition times at the ms level. If this is true, it explains why pulses with t_p and t_r of 0.1 s each give a much higher hybridization efficiency than pulses lasting 1 s or the constantly applied potential. Under these conditions, surface-tethered DNA capture probes are not too long "trapped" in either of the two electrostatics states discussed above.

The externally applied potential and its mode of application (constant vs pulses) is not the only factor that affects DNA hybridization. It is apparent that the ionic strength in the hybridization solution plays a crucial role. Hybridization efficiency at low ionic strength is very poor even when the external potential is applied. As has been pointed out by Levicky and others, the onset of hybridization is expected when the ion concentration in the bulk of the solution is equal or higher than the concentration of ions within the DNA layer.[13] Inseting target DNA molecules from solutions of the low ionic strength leads to a high entropy penalty because this transfer occurs uphill against the ion concentration gradient. The situation further aggravates at high Γ_{max} when the concentration gradient between surface-confined ions and bulk increases. At the same time, it is supposed here, that surface hybridization is controlled by the chemical step (the duplex nucleation) not the diffusional transport of DNA molecules from the bulk toward the surface, due to the high excess of target molecules compared to the number of adsorption sites. Taking into account the surface probe concentration and the target concentration and a diffusion coefficient of DNA of $D \approx 1 \times 10^{-6}$ cm^2/s, the association time (τ) eq 1 is on the range of 70 s for the reaction under diffusion control. Association times obtained from fitting data to first-order Langmuir isotherm are in the range of 200−800 s. That means that hybridization reactions presented in this work are truly under chemical control. Therefore, in our opinion, no effect on hybridization can arise from enhanced DNA transport such as electrophoretic migration that should be stronger at low ionic strength. This distinguishes our results from other studies aiming to enhancing surface DNA hybridization by the generation of an electric field at the electrode.[29,30] In most of these studies, high potentials in the range of few V had been applied to the electrode surfaces. This ensures conditions similar to gel electrophoresis, where transport of DNA molecules by electrophoretic forces plays a major role in enhancing the DNA surface hybridization.

5. CONCLUSIONS

Electrochemical studies on potential-assisted DNA surface hybridization at the regime of high capture probe density were presented. The normally suppressed hybridization for such monolayers could be at least partially restored by generating a positive electric field at the interface that mitigates the electrostatic barrier responsible for impeding hybridization. We observed that pulsing the applied potentials between +50 mV and +300 mV at an appropriate frequency resulted in faster hybridization kinetics and improved hybridization efficiency as compared to applying a constant potential. Hybridization kinetics was treated in terms of a first-order Langmuir adsorption isotherm. Though high-density monolayers do not meet requirements of the first-order Langmuir isotherm because of significant intermolecular interaction, for the purpose of this study, this treatment serves sufficient approximation. The obtained results using EIS and FSCV together with Fc-tagged target DNA strands were consistent with previous studies showing increased hybridization efficiency for high-density DNA monolayers upon applying an external potential that increases the association rate constant to a level similar as for diluted monolayers.

AUTHOR INFORMATION

Corresponding Author

*E-mail: magdalena.gebala@rub.de or mgebala@stanford.edu.

Present Address

[†]M.G. is currently at Department of Biochemistry, Stanford University, Stanford, CA 94305, United States.

Author Contributions

The manuscript was written through contributions of all authors. All authors have given approval to the final version of the manuscript.

Notes

The authors declare no competing financial interest.

ACKNOWLEDGMENTS

The authors are grateful to the research department interfacial systems chemistry (RD-IFSC) at the Ruhr-Universität Bochum and to the BMBF in the framework of the projects "PathogenDirekt" (FKZ: 0315823B) and "UriproC" (FKZ: 03SHWB033).

REFERENCES

(1) Millan, K. M.; Mikkelsen, S. R. Sequence-Selective Biosensor for DNA Based on Electroactive Hybridization Indicators. *Anal. Chem.* **1993**, *65*, 2317−2323.

(2) Drummond, T. G.; Hill, M. G.; Barton, J. K. Electrochemical DNA Sensors. *Nat. Biotechnol.* **2003**, *21*, 1192−1199.

(3) Gebala, M.; Stoica, L.; Guschin, D.; Stratmann, L.; Hartwich, G.; Schuhmann, W. A Biotinylated Intercalator for Selective Post-Labeling of Double-Stranded DNA as a Basis for High-Sensitive DNA Assays. *Electrochem. Commun.* **2010**, *12*, 684−688.

(4) Li, D.; Zou, X.; Shen, Q.; Dong, S. Kinetic Study of DNA/DNA Hybridization with Electrochemical Impedance Spectroscopy. *Electrochem. Commun.* **2007**, *9*, 191−196.

(5) Kafka, J.; Paenke, O.; Abendroth, B.; Lisdat, F. A Label-Free DNA Sensor Based on Impedance Spectroscopy. *Electrochim. Acta* **2008**, *53*, 7467−7474.

(6) Keighley, S. D.; Estrela, P.; Li, P.; Mighorato, P. Optimization of Label-Free DNA Detection with Electrochemical Impedance Spectroscopy Using PNA Probes. *Biosens. Bioelectron.* **2008**, *24*, 906−911.

(7) Gebala, M.; Stoica, L.; Neugebauer, S.; Schuhmann, W. Label-Free Detection of DNA Hybridization in Presence of Intercalators Using Electrochemical Impedance Spectroscopy. *Electroanal.* **2009**, *21*, 325−331.

(8) Gebala, M.; Schuhmann, W. Controlled Orientation of DNA in a Binary SAM as a Key for the Successful Determination of DNA Hybridization by Means of Electrochemical Impedance Spectroscopy. *ChemPhysChem* **2010**, *11*, 2887−2895.

(9) Peterson, A. W.; Heaton, R. J.; Georgiadis, R. M. The Effect of Surface Probe Density on DNA Hybridization. *Nucleic Acids Res.* **2001**, *29*, 5163−5168.

(10) Vainrub, A.; Pettitt, B. M. Surface Electrostatic Effects in Oligonucleotide Microarrays: Control and Optimization of Binding Thermodynamics. *Biopolymers* **2003**, *68*, 265−270.

(11) Erickson, D.; Li, D.; Krull, U. Modeling of DNA Hybridization Kinetics for Spatially Resolved Biochips. *Anal. Biochem.* **2003**, *317*, 186−200.

(12) Castelino, K.; Kannan, B.; Majumdar, A. Characterization of Grafting Density and Binding Efficiency of DNA and Proteins on Gold Surfaces. *Langmuir* **2005**, *21*, 1956−1961.

(13) Gong, P.; Levicky, R. DNA Surface Hybridization Regimes. *Proc. Natl. Acad. Sci. U.S.A.* **2008**, *105*, 5301−5306.

(14) Wong, I. Y.; Melosh, N. A. An Electrostatic Model for DNA Surface Hybridization. *Biophys. J.* **2010**, *98*, 2954−2963.

(15) Heller, M. J.; Forster, A. H.; Tu, E. Active Microelectronic Chip Devices which Utilize Controlled Elerophoretic Field for Multiplex DNA Hybridization and Other Genomic Applications. *Electrophoresis* **2000**, *21*, 157−164.

(16) Heaton, R. J.; Peterson, A. W.; Georgiadis, R. M. Electrostatic Surface Plasmon Resonance: Direct Electric Field-Induced Hybridization and Denaturation in Monolayer Nucleic Acid Films and Label-Free Discrimination of Base Mismatches. *Proc. Natl. Acad. Sci. U.S.A.* **2001**, *98*, 3701−3704.

(17) Fixe, F.; Branz, H. M.; Louro, N.; Chu, V.; Prazeres, D. M. F.; Conde, J. P. Electric-Filed Assisted Immobilization and Hybridization of DNA Oligomers on Thin-Film Microchips. *Nanotechnology* **2005**, *16*, 2061−2071.

(18) Wong, I. Y.; Melosh, N. A. Directed Hybridization and Melting of DNA Linkers Using Counterion-Screened Electric Fields. *Nano Lett.* **2009**, *9*, 3521−3526.

(19) Cabeca, R.; Rodrigues, M.; Prazeres, D. M. F.; Chu, V.; Conde, J. P. The Effect of the Shape of Single, Sub-ms Voltage Pulse on the Rates of Surface Immobilization and Hybridizaiton of DNA. *Nanotechnology* **2009**, *20*, 015503.

(20) Peterson, E. M.; Harris, J. M. Single-Molecule Fluorescence Imaging of DNA at a Potential-Controlled Interface. *Langmuir* **2013**, *29*, 8292−8301.

(21) Gebala, M.; La Mantia, F.; Schuhmann, W. Kinetic and Thermodynamic Hysteresis Imposed by Intercalation of Proflavine in Ferrocene-Modified Double-Stranded DNA. *ChemPhysChem* **2013**, *14*, 2208−2216.

(22) Kuznetsov, V.; Papastavrou, G. Ion Adsorption on Modified Electrodes as Determined by Direct Force Measurements under Potentiostatic Control. *J. Phys. Chem. C* **2014**, *118*, 2673−2685.

(23) Anne, A.; Demaille, C. Electron Transport by Molecular Motion of Redox-DNA Strands: Unexpectedly Slow Rotational Dynamics of 20-mer ds-DNA Chains End-Grafted onto Surfaces via C(6) Linkers. *J. Am. Chem. Soc.* **2008**, *130*, 9812−9823.

(24) Anne, A.; Demaille, C. Dynamics of Electron Transport by Elastic Bending of Short DNA Duplexes. Experimental Study and Quantitative Modeling of the Cyclic Voltammetric Behavior of 3′-Ferrocenyl DNA End-Grafted on Gold. *J. Am. Chem. Soc.* **2006**, *128*, 542−557.

(25) Hüsken, N.; Gebala, M.; Battistel, A.; La Mantia, F.; Schuhmann, W.; Metzler-Nolte, N. Impact of Single Basepair Mismatches on Electron-Transfer Processes at Fc-PNA·DNA Modified Gold Surfaces. *ChemPhysChem* **2012**, *13*, 131−139.

(26) Halperin, A.; Buhot, A.; Zhulina, E. B. Brush Effects on DNA Chips: Thermodynamics, Kinetics, and Design Guidelines. *Biophys. J.* **2005**, *89*, 769−811.

(27) Rant, U.; Arinaga, K.; Scherer, S.; Pringsheim, E.; Fujita, S.; Yokoyama, N.; Tornow, M.; Abstreiter, G. Switchable DNA Interfaces for the Highly Sensitive Detection of Label-Free DNA Targets. *Proc. Natl. Acad. Sci. U.S.A.* **2007**, *104*, 17364−17369.

(28) Rant, U.; Arinaga, K.; Tornow, M.; Kim, Y. W.; Netz, R. R.; Fujita, S.; Yokoyama, N.; Abstreiter, G. Dissimilar Kinetic Behavior of Electrically Manipulated Single- and Double-Stranded DNA Tethered to a Gold Surface. *Biophys. J.* **2006**, *90*, 3666−3671.

(29) Sosnowski, R. G.; Tu, E.; Butler, W. F.; O'Connell, J. P.; Heller, M. J. Rapid Determination of Single Base Mismatch Mutations in DNA Hybrids by Direct Electric Field Control. *Proc. Natl. Acad. Sci. U.S.A.* **1997**, *94*, 1119−1123.

(30) Edman, C. F.; Raymond, D. E.; Wu, D. J.; Tu, E.; Sosnowski, R. G.; Butler, W. F.; Nerenberg, M.; Heller, M. Electric Field Directed Nucleic Acid Hybridization on Microchips. *Nucleic Acids Res.* **1997**, *25*, 4907−4914.